DALTON
FULL PAPER

Formation of dinuclear macrocyclic and mononuclear acyclic complexes of a new trinucleating hexaaza triphenolic Schiff base macrocycle: structure and NLO properties

Srinivas R. Korupoju,[a] Nagarathinam Mangayarkarasi,[a] Sardar Ameerunisha,[a] Edward J. Valente[b] and Panthappally S. Zacharias[a]

[a] *School of Chemistry, University of Hyderabad, Hyderabad 500 046, India*
[b] *Department of Chemistry, Mississippi College, Clinton, MS 39058, USA*

Received 5th April 2000, Accepted 3rd July 2000
Published on the Web 2nd August 2000

Reaction of a new chiral and optically active trinucleating 3 + 3 condensed hexaaza triphenolic Schiff base macrocycle H_3L^1 **I** with transition metal ions (Zn, Cu, Ni, Co, Fe and Mn) in 1 : 3 molar ratio in methanol under reflux conditions resulted in complexes. Analytical data reveal the formation of 2 + 2 condensed dinuclear macrocyclic Schiff base complexes, instead of the expected trinuclear macrocyclic complexes. X-Ray crystallographic studies on three of these complexes established their dinuclearity. On the other hand, reaction of **I** with metal ions (Zn, Cu, Fe and Mn) in 1 : 3 molar ratio in methanol at room temperature for 2 h resulted in one-side condensed mononuclear acyclic complexes. This is confirmed by the crystal structure of the manganese complex. Second-order non-linear properties are discussed.

Introduction

Polynuclear systems with three or more metal ions bridged by oxo and acetato groups have recently attracted considerable attention due to the existence of oxo-bridged tri- and multinuclear metal constellations in metalloproteins and enzymes.[1–5] The presence of trinuclear active sites in enzymes has been established by crystal structures. Synthesis of model complexes can be achieved by the self assembly of simple ligands but the reproducibility is less compared to other methods.[6] Alternatively preformed ligands are useful for these syntheses in addition to their utility in reactions with metals inert to template reactions.[7]

2,6-Diformyl-4-methylphenol (dfp) is a potential precursor to synthesize mono- and multi-nucleating acyclic and macrocyclic ligands.[8–12] Condensation of dfp with diamines in the presence of template 3d metal ions generates predominantly 2 + 2 oxo-bridged dinuclear complexes. The metal–metal cooperative effects and consequent physico-chemical and biocatalytic properties of these complexes have been studied extensively.[9] By altering the reaction conditions like solvent and temperature a few 3 + 3 hexanuclear and 4 + 4 tetranuclear macrocyclic complexes were isolated.[10] With H^+ ion as a template, 2 + 2 condensed metal-free macrocycles were the predominant products.[11] Attempts to synthesize template-free macrocycles with dfp gave polymers and oligomers as major products but in a few instances 1 + 1 and 3 + 2 macrocyclic ligands were isolated.[12]

Recently we have reported the first template-free, trinucleating 3 + 3 Schiff base macrocycle H_3L^1 **I** from the condensation of dfp and *trans*-(1*R*,2*R*)-cyclohexanediamine.[13] Applications of chiral and optically active *trans*-1,2-cyclohexanediamine derivatives and their complexes as stereoselective catalysts for organic reactions[14] prompted the choice of this diamine in dfp chemistry. The molecular structure of **I** has been deduced from the crystal structure of its reduced analogue **II**. The trinucleating ability of the macrocycle **II** has been demonstrated by the X-ray structural characterization of its zinc complex $[Zn_3L^2(\mu\text{-OAc})]^{2+}$.[15] Anticipating the formation of trinuclear complexes, the ligand **I** was treated with 3d metal ions (Zn, Cu, Ni, Co, Fe and Mn) which resulted in 2 + 2 condensed dinuclear macrocyclic complexes under reflux conditions and acyclic mononuclear Schiff base complexes at room temperature (Scheme 1). Here we discuss the details of the synthesis and X-ray structural characterization of these two types of complexes.

Results and discussion

Synthesis and characterization of ligand H_3L^1, I

The reaction of dfp and *trans*-(1*R*,2*R*)-cyclohexanediamine gave the 3 + 3 condensed Schiff base macrocyclic ligand **I** as a yellow solid in high yields. The molecular ion peak at *m*/*z* 727 in the FAB mass spectrum confirms the 3 + 3 condensation. The molecular structure has been established from the analytical data and the crystal structure of its reduced analogue H_3L^2, **II**.[13] The formation of the 3 + 3 macrocycle is probably due to the optimum ring size and kinetic and thermodynamic stability. It consists of three equivalent N_2O_2 sub-groups, which can facilitate the binding of three metal ions in close proximity through oxo-bridges.

Dinuclear complexes

With the objective to synthesize trinuclear complexes of macrocycle **I**, it was treated with transition metal ions (Mn to Zn) in 1 : 3 molar ratio in methanol under refluxing conditions which resulted in the formation of complexes **1**–**6** (see Experimental section). The IR stretching bands of **1**–**6** at around 1635 and 1545 cm^{-1} suggest the presence of C=N and M–O–M groups respectively. The anions $CH_3CO_2^-$ and ClO_4^- are identified with their characteristic peaks at 1390–1430, 1090 and 625 cm^{-1}. The CHN analytical data of the complexes do not agree with the expected trinuclear composition but match with the composition of 2 + 2 dinuclear macrocyclic complexes. The molecular ion peak at around *m*/*z* 700 in the FAB mass spectra of the complexes suggests the formation of dinuclear macrocyclic complexes. The IR, CHN and FAB mass spectral data are consistent with a dinuclear composition (see Experimental section). The electronic spectra of the complexes exhibit

DOI: 10.1039/b002700f

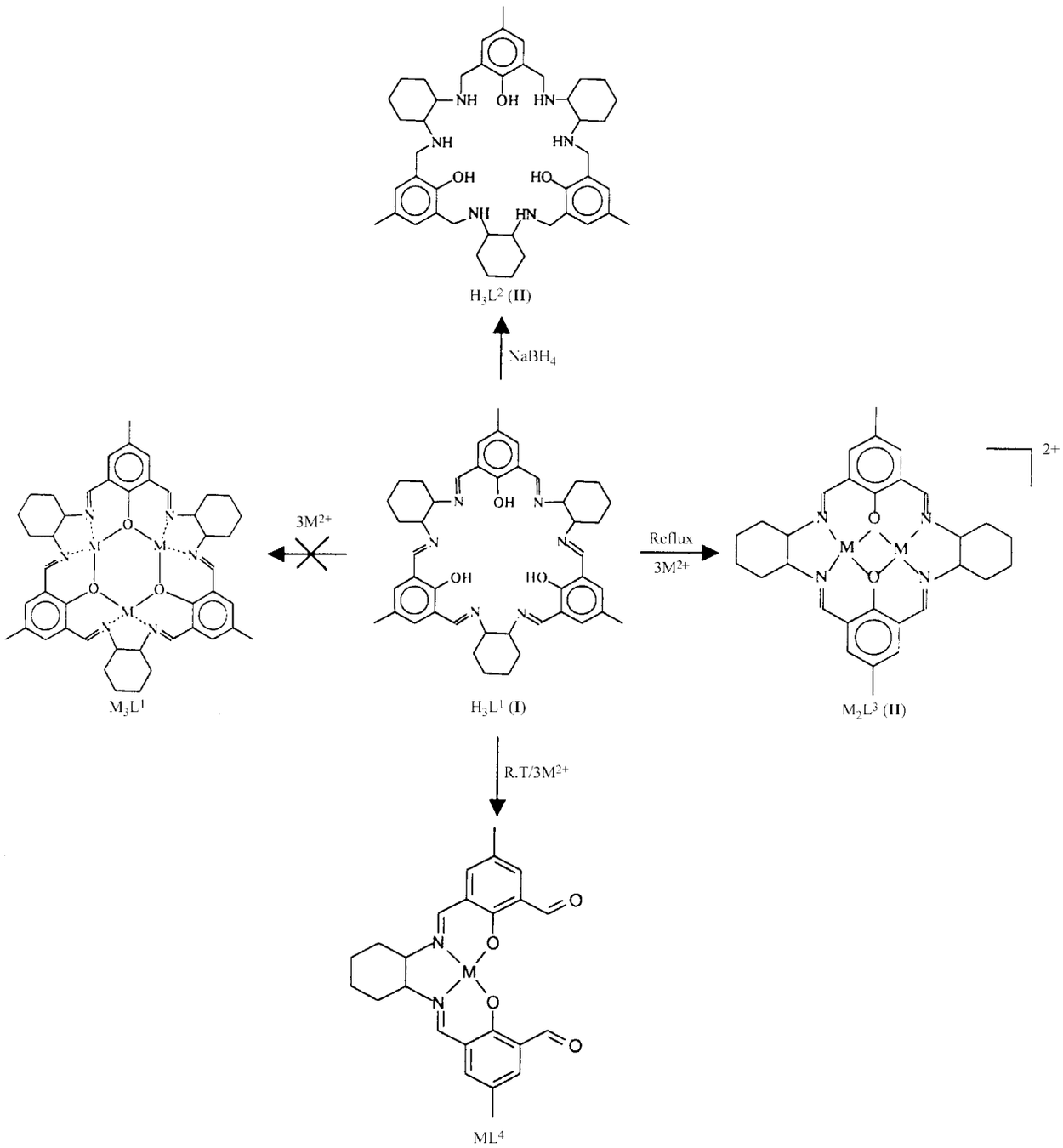

Scheme 1 Product formation pattern of macrocycle **I**.

absorption bands at around 255 nm due to intraligand π–π* transitions. The bands at around 364–450 nm may be due to metal to ligand charge transfer transitions. The molecular structures of the complexes were confirmed for **1**, **2** and **3**. Selected bond lengths and angles are listed in Tables 1 and 2.

$[Zn_2L^3Cl_2]$, 1. The ^{1}H NMR spectrum of complex **1** shows one signal for azomethine protons at δ 8.3 and one signal for aryl protons at δ 7.3 as against the two signals observed for each of these protons in macrocycle **I**. The ^{13}C NMR spectrum supports this observation. The complex shows a strong absorption band at 399 nm and a shoulder band at 455 nm (in CH_3CN) due to the ligand to metal charge transfer transition. The analytical and spectral data suggest a dinuclear structure for the complex which is confirmed by the X-ray crystal structure.

Crystallization of the complex **1** on slow evaporation of solvent $CHCl_3$–CH_3CN (1 : 1) gave stable yellow rhombic crystals suitable for X-ray crystallography. The complex crystallizes in monoclinic $P2_1$ space group. The asymmetric unit consists of one molecule with the composition $[Zn_2L^3Cl_2]$. An ORTEP[16] diagram of the complex with atom labeling is shown in Fig. 1. Selected bond lengths and angles are given in Tables 1 and 2. The co-ordination geometry at each metal atom may be regarded as distorted square pyramidal bridged by two oxo-groups, with two imine nitrogens in the basal plane and the chloride anion in the axial position. The macrocycle has a planar form and the two cyclohexyl rings of the ligand are in chair form. The zinc atom lies out of the N_2O_2 basal plane by 0.7901 (Zn1) and 0.7816 Å (Zn2) respectively. The zinc(II)–imine nitrogen (≈ 2.06 Å) and –oxygen (≈ 2.01 Å) bond distances are in the range observed for similar dinuclear C_3 side chain macrocyclic complexes. The observed Zn(1)–O(1)–Zn(2) and Zn(1)–O(2)–Zn(2) angles are 104.6(3) and 104.3(2)°. The Zn(1)···Zn(2), Zn(1)–Cl(1) and Zn(2)–Cl(2) distances are 3.19, 2.246(2) and 2.229(2) Å. Intermolecular C–H···Cl interactions are observed between the C–H protons of the

Table 1 Selected bond distances (Å) and angles (°) of complexes **1**, **2**, **3** and **7**

1		**2**		**3**		**7**	
Zn(1)···Zn(2)	3.19	Cu(1)···Cu(2)	2.87	Ni(1)···Ni(2)	2.808(15)	Mn1···Mn1	6.9138
Zn(1)–O(1)	2.057(6)	Cu(1)–O(3)	1.915(7)	Ni(1)–O(1)	1.833(8)	Mn2···Mn2	6.8789
Zn(1)–O(2)	2.052(5)	Cu(1)–O(4)	1.922(7)	Ni(1)–O(2)	1.860(8)	Mn1···O1W	2.311(15)
Zn(2)–O(1)	1.975(6)	Cu(2)–O(3)	1.922(7)	Ni(2)–O(1)	1.821(8)	Mn1···O1	1.895(14)
Zn(2)–O(2)	1.989(6)	Cu(2)–O(4)	1.918(7)	Ni(2)–O(2)	1.837(8)	Mn1···N1	2.033(14)
Zn(1)–N(1)	2.070(7)	Cu(1)–N(1)	1.886(8)	Ni(1)–N(3)	1.822(8)	Mn2···N2	1.91(2)
Zn(1)–N(2)	1.994(6)	Cu(2)–N(2)	1.904(8)	Ni(1)–N(4)	1.824(9)	Mn2···O2W	2.205(15)
Zn(2)–N(3)	2.076(7)	Cu(2)–N(3)	1.894(8)	Ni(2)–N(1)	1.797(9)	Mn2···O3	1.860(13)
Zn(2)–N(4)	2.120(7)	Cu(1)–N(4)	1.895(8)	Ni(2)–N(2)	1.826(8)		
Zn(1)–Cl(1)	2.246(2)	Cu(1)–O(2)	2.159(8)				
Zn(2)–Cl(2)	2.229(2)	Cu(2)–O(1)	2.156(8)				
Zn(1)–O(1)–Zn(2)	104.6(3)	Cu(1)–O(3)–Cu(2)	97.0(3)	Ni(1)–O(1)–Ni(2)	100.4(4)	O1–Mn1–N1	93.1(5)
Zn(1)–O(2)–Zn(2)	104.3(2)	Cu(1)–O(4)–Cu(2)	96.8(3)	Ni(1)–O(2)–Ni(2)	98.9(4)	O1–Mn1–O1#1	92.6(8)
N(1)–Zn(1)–N(2)	83.1(3)	N(1)–Cu(1)–N(4)	88.9(4)	N(3)–Ni(1)–N(4)	88.9(4)	N1–Mn1–N1#1	81.3(8)
N(3)–Zn(2)–N(4)	80.8(3)	N(2)–Cu(2)–N(3)	88.2(4)	N(1)–Ni(2)–N(2)	89.1(4)	O3–Mn2–N2	93.0(7)
N(2)–Zn(1)–O(2)	86.2(3)	N(1)–Cu(1)–O(3)	92.0(3)	N(3)–Ni(1)–O(2)	95.8(4)	O3–Mn2–O3#2	91.4(8)
N(1)–Zn(1)–O(1)	82.3(3)	N(3)–Cu(2)–O(4)	92.4(4)	N(4)–Ni(1)–O(1)	96.4(4)	N2–Mn2–N2#2	82.6(12)
N(3)–Zn(2)–O(2)	85.0(2)	N(4)–Cu(1)–O(4)	91.9(4)	N(2)–Ni(2)–O(2)	94.9(4)		
N(4)–Zn(2)–O(1)	83.6(3)	N(2)–Cu(2)–O(3)	92.4(4)	N(1)–Ni(2)–O(1)	95.5(4)		

Table 2 Geometrical parameters of intermolecular interactions of complexes **1**, **2** and **3**

Complex	Interaction	C–H/Å	D^a/Å	d^b/Å	θ^c/°
1	C(12)–H(12A)···Cl(2)	0.9701	3.6407	2.7839	147.67
2	C(11)–H(11C)···Cu(1)	0.961(2)	3.924(2)	3.101(2)	144.8(2)
	C(7)–H(7A)···O(3A)	0.930(2)	3.430(2)	2.528(2)	164.0(2)
	C(20)–H(20A)···O(1)	0.930(2)	3.348(2)	2.470(2)	157.8(2)
	C(22)–H(22A)···O(2)	0.930(2)	3.357(2)	2.563(2)	143.8(2)
3	C(6)–H(6)···O(10)	0.9300	3.3277	2.4189	165.57
	C(8)–H(8)···O(8)	0.9300	3.3041	2.4994	144.94
	C(15)–H(15)···O(10)	0.9800	3.4085	2.5982	140.10
	C(18)–H(18)···O(6)	0.9300	3.4380	2.5642	156.69
	C(24)–H(24)···O(3)	0.9299	3.3453	2.5070	150.08

[a] The distance between C and the acceptor (Cl or O). [b] The distance between H and the acceptor (Cl or O). [c] The angle at H in C–H···X (X = Cl or O).

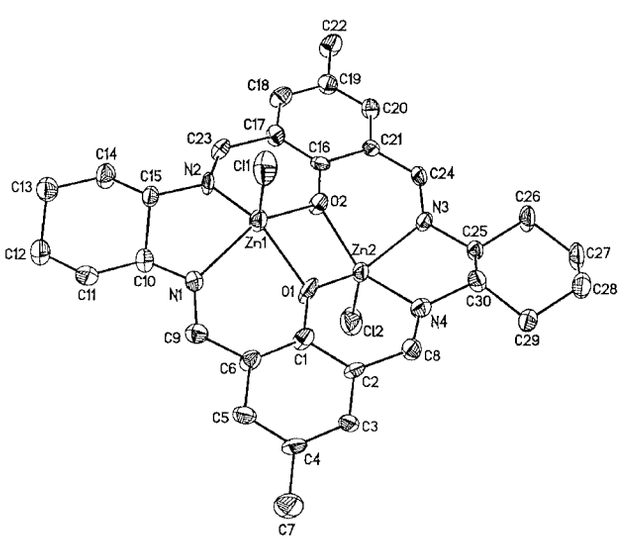

Fig. 1 An ORTEP diagram of complex $[Zn_2L^3Cl_2]$, **1** showing 35% probability thermal ellipsoids (as in all cases).

cyclohexyl group and the Cl(2) of another molecule with a distance of 2.78 Å [C(12)–H(12A)···Cl(2), D = 3.6407 Å, d = 2.7839 Å, θ = 147.67°]. On the other hand, Cl(1) has long range intermolecular interaction [C(28)–H(28A)···Cl(1), d = 3.317 Å] (Table 2).

Though dinuclear zinc macrocyclic complexes of dfp and 1,3-diaminopropane have been crystallographically characterized,[17] this is the first report on the structure of dinuclear complexes with C_2 side chain diamines.

$[Cu_2L^3(\mu\text{-OAc})]ClO_4\cdot CH_3CN$, 2. The analytical, IR and spectral data of complex **2** are given in the Experimental section. The shoulder band in the visible region at 545 nm is due to metal d–d electronic transitions and suggests square pyramidal geometry around the copper centers. Similar bands have been observed for several analogous oxo-bridged copper complexes.[9] The proposed dinuclear structure of the complex is confirmed crystallographically.

Recrystallization of complex **2** from CH_3OH–CH_3CN (1 : 1) gave orange-brown rhombic crystals suitable for X-ray crystallography. The complex crystallizes in monoclinic space group $P2_1/c$. The asymmetric unit consists of one molecule with the composition of $[Cu_2L^3(\mu\text{-OAc})]ClO_4\cdot CH_3CN$. The ORTEP diagram of **2** is shown in Fig. 2. The crystal structure shows that the two copper centers adopt a distorted square pyramidal geometry, each being co-ordinated by two imino nitrogens, two phenoxy bridging oxygens in the basal plane and bridged by an acetate group in an axial position. The Cu(1) and Cu(2) are displaced from the N_2O_2 basal plane by 0.3323 and 0.3325 Å respectively towards the acetate oxygens. The Cu(1)–O(3)–Cu(2) and Cu(1)–O(4)–Cu(2) angles are 97.0(3) and 96.8(3)° and the intermetallic Cu(1)···Cu(2) distance is 2.872(2) Å. The distances of the axial acetate oxygen atoms from the metal ions are Cu(1)–O(2) 2.159(8) and Cu(2)–O(1) 2.156(8) Å. The Cu(1) has long range axial co-ordination through weak intermolecular interaction with the proton of the *p*-methyl group at a distance of 3.10 Å. The C_2 linkage between the imine groups and two other carbon atoms of the ring is disordered over two sites with occupancies of 0.49 and 0.51. The complex shows intermolecular C–H···O hydrogen bonding between the aromatic protons

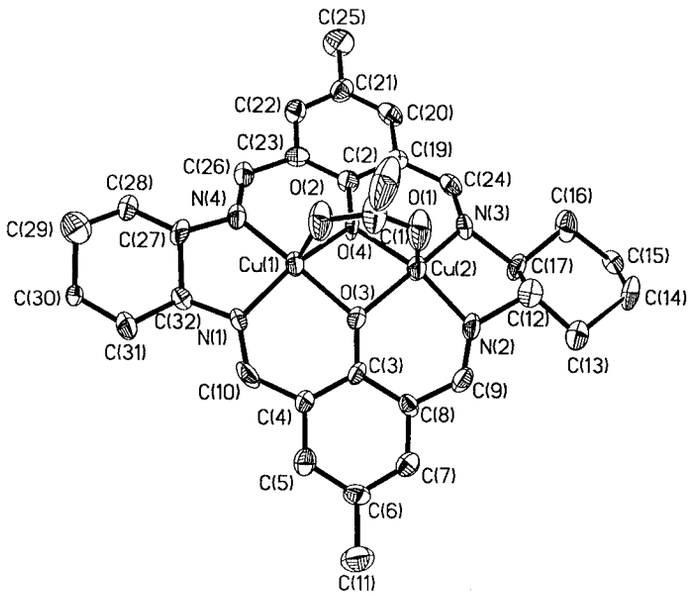

Fig. 2 An ORTEP diagram of complex $[Cu_2L^3(\mu\text{-}OAc)]^+$, **2**.

and the oxygens of bridging acetate groups in the range of 2.47 to 2.56 Å (Table 2).

Molecular structures of analogous 2 + 2 dinuclear copper Schiff base macrocyclic complexes with C_2 side chain diamines were established crystallographically.[8,9,18] In C_2 side chain complexes, when the metal centers are bridged by acetate and perchlorate groups the Cu···Cu distance is in the range of 2.84 to 2.88 Å and in the case of non-bridging anions the distances are around 2.90–2.94 Å. In the case of analogous C_3 side chain complexes the Cu···Cu distance lies in the range of 3.03 to 3.36 Å.[9]

In acetonitrile with a glassy carbon working electrode, complex **2** shows two stepwise one-electron reductions at −0.63 and −1.25 V corresponding to $Cu^{II}Cu^{II}L^3$–$Cu^{II}Cu^{I}L^3$ and $Cu^{II}Cu^{I}L^3$–$Cu^{I}Cu^{I}L^3$. Similar behaviour is observed for analogous dinuclear copper(II) complexes. The room temperature magnetic moment of 1.25 μ_B indicates strong antiferromagnetic interaction between the metal centers.

$[Ni_2L^3][ClO_4]_2\cdot CH_3CN\cdot CH_3OH$, 3. The electronic spectrum of complex **3** exhibits a shoulder band at 576 nm due to metal d–d electronic transition, assigned to $^1A_1(F) \longrightarrow {}^1B_1$. Such a band is observed for four-co-ordinate square planar nickel complexes.[19] The dinuclear structure of the complex is confirmed crystallographically.

Complex **3** crystallizes in monoclinic space group $P2_1/c$. The asymmetric unit consists of one molecule. The ORTEP diagram of the complex is shown in Fig. 3. The nickel ion environment is square planar generated by two imine nitrogens and two bridging oxygen atoms of the ligand. The Ni(1)–O(1)–Ni(2) and Ni(1)–O(2)–Ni(2) angles are 100.4 and 98.9°. The nickel ions lie in the plane of the N_2O_2 compartment and the Ni(1)···Ni(2) distance is 2.80 Å. The cyclohexane rings are in chair conformation. Complex **3** has two unco-ordinated perchlorate anions, one methanol and an acetonitrile molecule in the crystal lattice. Weak intermolecular C–H···O hydrogen bonding between the aromatic and azomethine protons of the macrocycle and the perchlorate oxygens is observed. The distances of these bonds range from 2.41 to 2.59 Å (Table 2).

Complex **3** exhibits two stepwise quasi-reversible one-electron reduction peaks in the negative potential range at −0.72 and −1.32 V in acetonitrile corresponding to $Ni^{II}Ni^{II}L^3$–$Ni^{II}Ni^{I}L^3$ and $Ni^{II}Ni^{I}L^3$–$Ni^{I}Ni^{I}L^3$. At positive potentials it shows two quasi-reversible one electron oxidation peaks at +0.67 and +1.37 V respectively corresponding to stepwise

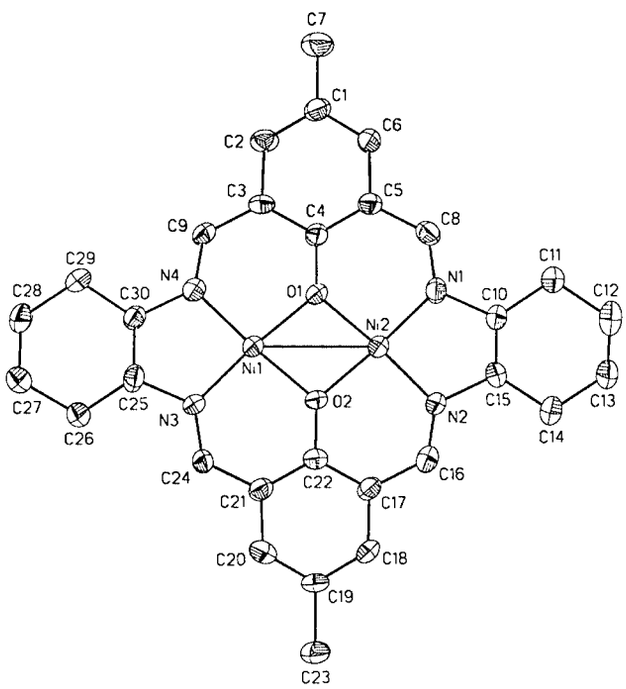

Fig. 3 An ORTEP diagram of complex $[Ni_2L^3]^{2+}$, **3**.

oxidation. Differential pulse voltammetry reveals the occurrence of two equal peaks at positive potentials that show the stabilization of the Ni^{3+} oxidation state. This has not been reported for dinuclear Schiff base nickel complexes of dfp.[19] Their reduced tetraamino analogues have been shown to stabilize the Ni^{3+} oxidation state.[20] Room temperature magnetic susceptibility shows the diamagnetic nature of the complex.

$[Co_2L^3][OAc]_2[ClO_4]_2$, 4. The elemental analysis of complex **4** suggests the molecular composition $[Co_2L^3][OAc]_2[ClO_4]_2$. A shoulder band appears at 619 nm due to metal d–d electronic transitions. Similar bands are observed for low spin octahedral cobalt(III) complexes.[21] The room temperature magnetic moment of the complex reveals a diamagnetic nature as expected for the low spin octahedral cobalt(III) geometry. Based on the spectral, magnetic properties and on comparison with analogous dinuclear cobalt complexes,[21] a dinuclear structure with distorted octahedral geometry is assigned. The cyclic voltam-

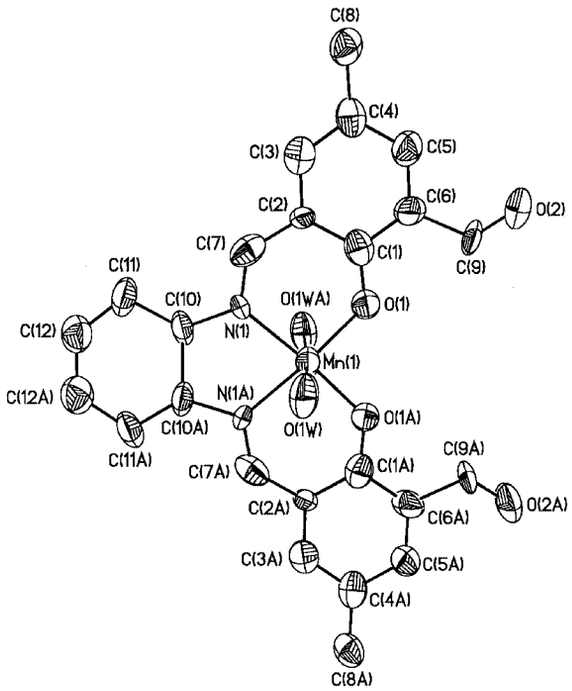

Fig. 4 An ORTEP diagram of complex $[MnL^4(OH_2)_2]^+$, **7**.

mogram of **4** exhibits two reduction waves at −0.11 and −1.02 V corresponding to successive one-electron reduction of cobalt ions from $Co^{III}Co^{III}L^3$–$Co^{III}Co^{II}L^3$ and $Co^{III}Co^{II}L^3$–$Co^{II}Co^{II}L^3$. The crystal structure was not determined since suitable crystals could not be obtained.

$[Fe_2L^3][OAc]_2[ClO_4]_2$, 5. The electronic spectrum of complex **5** shows a shoulder band at 856 nm due to the metal d–d transition. The cyclic voltammogram shows two quasi-reversible waves at −0.20 and −0.72 V for the successive reduction of two iron(III) ions to two Fe^{II} state. The DPV signals reveal the occurrence of two waves at the same potentials. The magnetic moment value for **5** at room temperature is 5.8 μ_B. Iron(III) high spin complexes either in octahedral or square-pyramidal geometry exhibit magnetic moments close to the spin only value of 5.92 μ_B. While it is difficult to differentiate between these two geometries from magnetic values,[22] on comparison with analogous dinuclear complexes a distorted octahedral geometry is proposed.

$[Mn_2L^3][ClO_4]_2$, 6. The electronic spectrum of complex **6** in acetonitrile did not show any d–d band in the visible region. CV exhibits two peaks in the negative potential at −0.20 and −1.23 V for the successive reduction of two metal ions. The room temperature magnetic moment is 5.8 μ_B, very close to 5.9 μ_B reported for dinuclear high spin octahedral manganese(II) Schiff base macrocyclic complexes.[23]

Mononuclear complexes

Several 2 + 2 dinuclear macrocyclic complexes have been isolated from the 2 + 2 metal-free macrocyclic ligands.[11] The formation of dinuclear complexes, **1**–**6**, from the trinucleating ligand **I** suggests metal assisted cleavage and rearrangement of the ligand. To probe this, an attempt was made to isolate the intermediate complexes. For this purpose the ligand **I** was treated with metal salts at room temperature for 2 h and the resultant complexes were isolated. Synthetic details and characterization data of **7**–**10** are given in the Experimental section. The characteristic IR spectral bands at ≈1666 and ≈1624 cm^{-1} reveal the presence of carbonyl and azomethine groups indicating cleavage of **I**. The CHN analysis of these complexes is consistent with one side condensed mononuclear Schiff base complexes. The FAB mass spectral ion peaks at *m*/*z* 467 and 460 of complexes **7** and **10** support the formation of mononuclear acyclic complexes. Based on the spectral, CHN and FAB mass spectral data, a mononuclear structure $[ML^4]^{n+}$ is proposed, where L^4 is the dianion of the acyclic Schiff base ligand. The electronic spectra of these complexes recorded in acetonitrile exhibit n–π* charge transfer bands at 367–398 nm. Metal d–d transitions are observed as shoulder bands in the range 515–590 nm. Analogous mononuclear complexes have been reported previously as intermediates in the synthesis of dinuclear Schiff base macrocyclic complexes using dfp.[24]

$[MnL^4(OH_2)_2]PF_6\cdot CH_3OH$, 7. To establish the structure of the complexes **7**–**10**, the crystal structure of **7** was determined. On slow evaporation of the solvent from the reaction solution at room temperature orange prismatic crystals suitable for X-ray crystallography were obtained. The complex crystallizes in orthorhombic space group *F*222 with the composition $[MnL^4(OH_2)_2]PF_6\cdot CH_3OH$. An ORTEP diagram with atom labeling is shown in Fig. 4.

The asymmetric unit has two crystallographically independent half molecules **A** and **B** with similar structure. There are eight such molecules in the unit cell. The crystallographic twofold axis passes through the metal and cyclohexyl moiety of the complex. The Mn atom has distorted octahedral geometry in molecules **A** and **B**. The two phenoxide oxygen and two C=N nitrogen atoms occupy the equatorial positions and the two water molecules are in axial positions. The Mn–O(1W) (water), Mn(1)–O(1) and Mn(1)–N(1) distances are 2.311(15), 1.895(14) and 2.003(14) Å respectively. The angles O(1)–Mn(1)–O(1#1) and N(1)–Mn(1)–N(1#1) are 92.6(8) and 81.3(8)°. The metal ion in molecule **B** has the same geometry and ligand environment as in molecule **A**. The bond distances and angles around Mn of **B** are generally less than those of **A**. The cyclohexyl rings of molecules **A** and **B** are packed in a ladder form. The solvent methanol is disordered and it assigned with site occupancy of 0.5 in the crystal lattice. The PF_6^- anion has disorder and was not refined further.

The band at 515 nm is due to the d–d electronic transition of low spin octahedral Mn^{III}. Complex **7** does not show any ESR signal in the solid state and in acetonitrile solution (from 303 to 145 K). One quasi-reversible peak at 0.02 V which corresponds to reduction of Mn^{III} to Mn^{II} is observed in the cyclic voltammogram.

Zinc, copper and iron complexes of H_2L^4. The zinc complex **8** was isolated as a yellow crystalline compound. The ^1H and ^{13}C NMR spectra along with the IR data confirm the presence of an aldehydic group. The CHN analytical data match the composition $ZnL^4(OH_2)_2$. The FAB mass spectral peak at *m*/*z* 467 and elemental analysis confirm the composition of the complex **9** as $[CuL^4]$. The cyclic voltammogram displays an irreversible wave at −0.776 V assigned to the reduction of $[Cu^{II}L^4]$ to $[Cu^{I}L^4]$. The room temperature magnetic moment value of 1.72 μ_B and the absorption band at 540 nm show distorted square planar geometry around copper(II). However, similar reactions with nickel and cobalt salts did not yield mononuclear complexes, but resulted in dinuclear complexes. For the iron complex, **10**, the room temperature magnetic moment of 5.6 μ_B and absorption band at 558 nm indicate the presence of high spin octahedral Fe^{III}. The cyclic voltammogram of the complex exhibits an irreversible signal at −1.00 V for the reduction of $Fe^{III}L^4$ to $Fe^{II}L^4$. A mononuclear structure similar to that of the manganese complex **7** is proposed for **8**–**10** by analogy. Crystal structures of these complexes were not determined since suitable crystals could not be obtained.

One side condensed ligands of dfp and 1,3-diaminopropane and their mononuclear copper and nickel complexes were

Table 3 Calculated AM1 second-order molecular hyperpolarizability (β) and experimental powder efficiency (χ^2)

Compound	$\beta/10^{-30}$ esu (calculated, λ 0.0 μm)	χ^2 (relative to urea, λ 1.0604 μm)
dfp	1.094	0.75
H_3L^1 **I**	3.325	0.10
H_2L^3	0.448	[a]
H_2L^4	1.529	[a]
$[Zn_2L^3Cl_2]$ **1**	7.066	0.90
$[Fe_2L^3][OAc]_2[ClO_4]_2$ **5**	[b]	0.75
$[ZnL^4(H_2O)_2]$ **8**	8.033	[c]

[a] H_2L^3 and H_2L^4 are generated structures. [b] Could not be calculated. [c] No experimental NLO response (χ^2).

reported earlier.[24] Also one side condensed mononuclear Schiff base copper and nickel complexes of 1,3,5-heptanetrione and ethylenediamine have been crystallographically characterized.[25] The reported mononuclear complexes and **7**–**10** have the metal ions in the N_2O_2 compartment and the carbonyl oxygens are free from any co-ordination.

Non-linear optical properties

Second-order non-linear optical (NLO) properties of molecular materials have attracted attention due to their application in the field of optoelectronics.[26] Compared to organic and organometallic systems,[27] very few studies have been reported on inorganic complexes. The donor–acceptor bis-(salicylaldiminato)metal complexes appear to be a promising family of efficient NLO chromophores.[28] Since many of these systems crystallize in a centrosymmetric or pseudocentrosymmetric environment, a vanishing bulk NLO response is observed. It was reported recently that the introduction of two asymmetric carbon atoms by the *trans*-cyclohexanediamine moiety into the compounds induced them to crystallize in a non-centrosymmetric space group which is a prerequisite for achieving a second order NLO response.[29]

Investigations on dfp and its complexes have been mostly on their physicochemical and catalytic properties and to a limited extent on the newly emerging field of optoelectronics. The π-electron delocalization and crystallization of dfp and its Schiff base compounds in a non-centrosymmetric space group prompted us to investigate the non-linear properties at the molecular (β) and bulk (χ^2) levels.

Preliminary second harmonic generation (SHG) measurements were carried out on powder samples at 1.064 μm using the Kurtz–Perry powder method[30] and urea as reference. These values are presented in Table 3. Fairly reliable second order molecular hyperpolarizability β was obtained for the ligands and the zinc complexes using semiempirical AM1 calculations (Table 3). The theoretical values indicate a sizable NLO response for this family of chromophores. In this case the phenolic proton acts as donor and C=O/C=N act as acceptor. The O–H · · · O/O–H · · · N hydrogen bond plays an important role in NLO. Comparison of dfp with its ligands and complexes shows a significant enhancement of β value except for the 2 + 2 Schiff base macrocycle.

dfp Crystallizes in the orthorhombic $P2_12_12_1$ space group. The powder SHG value for dfp is 0.75 times that of urea. That of macrocycle **I** is 0.10 times that of urea, whereas its calculated molecular hyperpolarizability (β) value shows an enhanced SHG activity in comparison to that of dfp. The dipole moment pathways in successive molecules may oppose each other, thus canceling the major part of β which results in relatively low powder efficiency (χ^2) of the above system.

Since the 2 + 2 Schiff base macrocycle has not been isolated the β value was calculated theoretically. The calculation predicts an enhancement of the NLO property after complexation. The complexes exhibit modest efficiency compared to that of the ligand, for example the powder SHG values of the dinuclear zinc and iron complexes are 0.90 and 0.75 times that of urea respectively. The copper and nickel complexes have a centrosymmetric space group and no NLO response was observed.

Conclusion

The crystal structures of complexes **1**, **2** and **3** demonstrate the formation of 2 + 2 dinuclear macrocyclic complexes resulting from cleavage and reorganization of the 3 + 3 macrocyclic ligand **I** during complexation. The reorganization of the ligand can be attributed to the planarity and thermodynamic stability of the 2 + 2 macrocyclic complex compared to that of the trinuclear macrocyclic complexes of ligand **I**. The geometry of the metal centers shows that these macrocyclic ligands stabilize five-co-ordinate distorted square pyramidal geometry around zinc and copper, whereas for nickel to manganese it stabilizes four-co-ordinate distorted square planar to six-co-ordinate distorted octahedral geometry. The crystal structure of the one side condensed mononuclear complex **7** adds further support to the cleavage of macrocycle **I**. The rearrangement to dinuclear macrocyclic complexes probably proceeds through the mononuclear complexes. Though the second order non-linear response of these molecules is modest, dfp, its Schiff base ligands and complexes represent a new class of stable materials for further NLO studies.

Experimental

Physical measurements

The elemental analyses of the compounds were carried out on a Perkin-Elmer 240C elemental analyzer. IR spectra were recorded on a JASCO FT/IR 5300 spectrometer in the range 4000–400 cm^{-1} in KBr pellets, electronic spectra on a JASCO model 7800 UV-VIS spectrophotometer (solution concentrations 1×10^{-3} mol dm^{-3} for the visible region and 1×10^{-5} mol dm^{-3} for the UV region) and NMR spectra on a Bruker ACF-200 spectrometer with TMS as internal standard. Magnetic susceptibility measurements were carried out by the Faraday method, at room temperature using a CAHN magnetic balance set-up. Diamagnetic corrections were made using Pascals' constants. Cyclic voltammograms were recorded on a Cypress systems model CS-1090/CS-1087 computer controlled electroanalytical system. All experiments were performed under dry nitrogen in solvents using 0.1 mol dm^{-3} NBu_4ClO_4 as supporting electrolyte, a glassy carbon working electrode, Ag–AgCl reference electrode and platinum wire as auxiliary electrode. The ferrocene–ferrocenium couple was used as the redox standard. Fast Atom Bombardment mass spectra were recorded on a JEOL SX 102/DA-6000 mass spectrometer/data system using xenon (6 kV, 10 mA) as the FAB gas and *m*-nitrobenzyl alcohol as the matrix.

Powder SHG measurements were carried out using the Kurtz–Perry technique[30] with the fundamental (1064 nm) of a Q-switched Nd:YAG laser. The powders were graded on the basis of the particle sizes using standard sieves and packed between glass plates. The sample thickness was maintained constant by measurement of uniform 0.2 mm thick Teflon sheets inserted as spacer between the glass plates. The SHG intensity was calibrated using powder samples of urea with particle size ≈150 μm. Samples showed no sign of decomposition even on prolonged irradiation with laser power of 1 GW cm^{-2} (6 ns, 10 Hz).

The computations were carried out using the MOPAC 93 program.[31] Molecular structure optimizations were carried out using the AM1 method[32] with the PRECISE keyword; full geometry relaxation was allowed. Theoretical analysis of the second order molecular hyperpolarizability (β) of compounds

Table 4 Crystallographic parameters of the dinuclear complexes **1**, **2**, **3** and **7**

	1	**2**	**3**	**7**
Empirical formula	$C_{30}H_{34}Cl_2N_4O_2Zn_2$	$C_{34}H_{40}ClCu_2N_5O_8$	$C_{33}H_{40}Cl_2N_5Ni_2O_{11}$	$C_{48}H_{48}F_{12}Mn_2N_4O_8P_2$
M	684.25	809.24	871.02	1008.81
Crystal system	Monoclinic	Monoclinic	Monoclinic	Orthorhombic
Space group	$P2_1$	$P2_1/c$	$P2_1/c$	$F222$
a/Å	8.740(8)	16.042(11)	9.00(3)	20.117(4)
b/Å	15.318(2)	19.769(9)	19.014(4)	58.207(12)
c/Å	11.285(4)	12.477(6)	11.518(4)	9.730(2)
β/°	105.34(4)	109.56(5)	106.33(12)	
U/Å^3, Z	1457.1(14), 2	3728(4), 4	1892, 2	11393(4), 8
μ/mm^{-1}	1.865	1.267	1.201	0.327
Reflections collected	2880	6341	3728	3611
Observed [$I > 2\sigma(I)$] reflections	2076	2226	2887	3589
Data, parameters	2652, 363	2226, 528	2887, 477	3589, 383
Final $R1$, $wR2$ [$I > 2\sigma(I)$]	0.0317, 0.0728	0.0835, 0.1809	0.0602, 0.1703	0.0821, 0.2380
(all data)	0.0461, 0.0804	0.2134, 0.2157	0.0701, 0.1831	0.2153, 0.2988

was made using AM1 semiempirical methods. The ligands H_2L^3, H_2L^4 were generated from the crystal structures of the dinuclear zinc and mononuclear manganese complexes respectively.

Synthesis of macrocycle I

2,6-Diformyl-4-methylphenol was prepared according to the literature method.[9] *trans*-(1*R*,2*R*)-Cyclohexanediamine was separated from the *cis*,*trans* mixture according to the literature procedure.[33]

To a solution of 2,6-diformyl-4-methylphenol (1.64 g, 10 mmol) in 100 cm^3 of methanol was added *trans*-(1*R*,2*R*)-cyclohexanediamine (1.14 g, 10 mmol) in 100 cm^3 of methanol. The reaction mixture was stirred vigorously at room temperature. The Schiff base macrocycle **I** separated as a yellow solid and the mixture was refluxed for 3 h and filtered. Yield 2.5 g (90%). $\tilde{\nu}_{max}$/cm^{-1} 1639 (C=N). δ_H(200 MHz, $CDCl_3$) 8.66 (3 H, s, HC=N), 8.2 (3 H, s, HC=N), 7.56 (3 H, s, ArH), 6.89 (3 H, s, Ar H), 3.3 (6 H, m, N–CH), 2.08 (9 H, s, Ar CH_3) and 1.86–1.46 (24 H, m, CH_2CH_2). δ_C(200 MHz, $CDCl_3$) 19.92, 24.45, 33.26, 33.48, 73.49, 75.45, 118.78, 122.99, 126.89, 129.56, 134.20, 156.15, 159.32 and 163.46. Found: C, 74.23; H, 7.46; N, 11.93%. Calc. for $C_{15}H_{18}N_2O$: C, 74.38; H, 7.43; N, 11.57%. *m*/*z* (%) 727 (100). $\alpha = -239°$ (589 nm, 30 °C, 10 gm dm^{-3} in DCM, 10 cm path length).

General synthetic procedure for complexes 1–6

The Schiff base **I** (0.33 mmol) in methanol (40 cm^3), $M(OAc)_2 \cdot nH_2O$ (0.5 mmol) in methanol (20 cm^3) and $M(ClO_4)_2 \cdot 6H_2O$ (0.5 mmol) in methanol (20 cm^3) were heated under reflux for 6 h. The reaction mixture was filtered and solvent evaporated on a rotavapor. The resulting crystalline complexes were washed with cold methanol and dried in air (yield ≈420 mg, 80%). They were recrystallized from methanol and acetonitrile. In the case of the iron complex $Na(OAc) \cdot 2H_2O$ and $Fe(ClO_4)_2 \cdot 6H_2O$ (1 : 3 : 3) were used. **CAUTION**: all perchlorates are prone to explosion and must be handled with care.

$[Zn_2L^3Cl_2]$, **1**: $\tilde{\nu}_{max}$/cm^{-1} 1635 and 1545. Found: C, 52.57; H, 5.08; N, 8.24%. Calc. for $C_{15}H_{17}ClN_2OZn$: C, 52.66; H, 5.00; N, 8.19%. λ_{max}/nm (ε/dm^3 mol^{-1} cm^{-1}) 455 (8520) and 399 (34780). $[Cu_2L^3(\mu\text{-}OAc)]ClO_4$, **2**: $\tilde{\nu}_{max}$/cm^{-1} 1635, 1545, 1091 and 625. Found: C, 49.89; H, 4.93; N, 7.35%. Calc. for $C_{32}H_{37}ClCu_2N_4O_8$: C, 50.00; H, 4.85; N, 7.29%. λ_{max}/nm (ε/dm^3 mol^{-1} cm^{-1}) 545 (466) and 364 (21000). *m*/*z* (%) 709 (40) and 608 (100). $[Ni_2L^3][ClO_4]_2$, **3**: $\tilde{\nu}_{max}$/cm^{-1} 1624, 1562, 1084 and 625. Found: C, 45.10; H, 4.35; N, 6.93%. Calc. for $C_{15}H_{17}ClN_2NiO_5$: C, 45.10; H, 4.29; N, 7.00%. λ_{max}/nm (ε/dm^3 mol^{-1}cm^{-1}) 576 (132) and 387 (15680). *m*/*z* (%) 698 (95) and 597 (100). $[Co_2L^3][OAc]_2[ClO_4]_2$, **4**: $\tilde{\nu}_{max}$/cm^{-1} 1637, 1566, 1097 and 625. Found: C, 44.47; H, 4.36; N, 6.10%. Calc. for $C_{17}H_{20}ClCoN_2O_7$: C, 44.51; H, 4.39; N, 6.11%. λ_{max}/nm (ε/dm^3 mol^{-1} cm^{-1}) 619 (608) and 366 (12440). $[Fe_2L^3][OAc]_2[ClO_4]_2$, **5**: $\tilde{\nu}_{max}$/cm^{-1} 1630, 1545, 1090 and 623. Found: C, 44.75; H, 4.39; N, 6.11%. Calc. for $C_{17}H_{20}ClFeN_2O_7$: C, 44.81; H, 4.42; N, 6.15%. λ_{max}/nm (ε/dm^3 mol^{-1} cm^{-1}) 856 (594) and 348 (26920). $[Mn_2L^3][ClO_4]_2$, **6**: $\tilde{\nu}_{max}$/cm^{-1} 1624, 1547, 1099 and 623. Found: C, 51.28; H, 5.21; N, 7.69%. Calc. for $C_{32}H_{37}ClMn_2N_4O_8$: C, 51.18; H, 4.97; N, 7.46%. λ_{max}/nm (ε/dm^3 mol^{-1} cm^{-1}) 445 (19540) and 402 (29260).

General synthetic procedure for complexes 7–10

The Schiff base **I** (0.33 mmol) in methanol (40 cm^3), $M(OAc)_2 \cdot nH_2O$ (0.5 mmol) in methanol (20 cm^3) and $M(ClO_4)_2 \cdot 6H_2O$ (0.5 mmol) and NH_4PF_6 (1 mmol) in methanol (20 cm^3) were stirred at room temperature for 2 h. In the case of iron only ClO_4^- and NH_4PF_6 salts were used. Slow evaporation of the solvent gave the crystalline complexes. They were washed with cold methanol and dried in air (yield ≈460 mg, 70%). Complex **7** gave crystals suitable for X-ray diffraction.

$[MnL^4]PF_6$, **7**: $\tilde{\nu}_{max}$/cm^{-1} 1666, 1626 and 837. Found: C, 47.63; H, 4.10; N, 4.70%. Calc. for $C_{24}H_{24}F_6MnN_2O_4P$: C, 47.70; H, 4.00; N, 4.64%. λ_{max}/nm (ε/dm^3 mol^{-1} cm^{-1}) 515 (1064) and 367 (8000). *m*/*z* (%) 460 (100). $[ZnL^4(H_2O)_2]$, **8**: $\tilde{\nu}_{max}$/cm^{-1} 1655 and 1624. Found: C, 56.92; H, 5.53; N, 5.53%. Calc. for $C_{24}H_{28}N_2O_6Zn$: C, 57.02; H, 5.58; N, 5.50%. λ_{max}/nm (ε/dm^3 mol^{-1} cm^{-1}) 448 (5820) and 378 (17840). $[CuL^4]$, **9**: $\tilde{\nu}_{max}$/cm^{-1} 1666 and 1633. Found: C, 61.52; H, 5.32; N, 6.13%. Calc. for $C_{24}H_{24}CuN_2O_4$: C, 61.60; H, 5.17; N, 6.00%. λ_{max}/nm (ε/dm^3 mol^{-1} cm^{-1}) 540 (258) and 391 (7720). $[FeL^4(H_2O)_2]PF_6$, **10**: $\tilde{\nu}_{max}$/cm^{-1} 1668, 1626 and 837. Found: C, 44.93; H, 4.37; N, 4.37%. Calc. for $C_{24}H_{24}F_6FeN_2O_4P$: C, 45.00; H, 4.31; N, 4.50%. λ_{max}/nm (ε/dm^3 mol^{-1} cm^{-1}) 558 (4750) and 360 (9116).

X-Ray crystallography

Crystals of complexes **1**, **2** and **3** were sealed in a glass capillary tube with mother liquor. For **1** and **3** data were collected on a MACH 3 Enraf Nonius cad4 diffractometer, for **2** and **7** using a Rigaku AFC7R diffractometer, with Mo-Kα radiation ($\lambda = 0.71073$ Å) at room temperature. Data reduction was done for **1** and **3** using XTAL version 3.5.[34] The structure was solved by direct methods using SHELX 97[34] and refined by full-matrix least-squares calculations on F^2. The structures of **2** and **7** were solved by direct methods using SHELXS and refined by full-matrix least-squares calculations on F^2 using SHELXTL 93.[34] Cell parameters were calculated from least-squares fitting of the setting angles for 25 reflections. Crystal data are summarized in Table 4.

CCDC reference number 186/2075.

See http://www.rsc.org/suppdata/dt/b0/b002700f/ for crystallographic files in .cif format.

Acknowledgements

S. R. K. and N. M. thank the University Grants Commission, New Delhi, India for financial support and Department of Science and Technology, New Delhi, India for the X-ray facility. We acknowledge Xue Feng and T. C. W. Mak, Department of Chemistry, Chinese University of Hong Kong for help in solving one crystal structure.

References

1 S. R. Collinson and D. E. Fenton, *Coord. Chem. Rev.*, 1996, **148**, 19; D. E. Fenton, in *Biocoordination Chemistry*, Oxford Science Publications, 1995; S. J. Lippard and J. M. Berg, in *Principles of Bioinorganic Chemistry*, University Science Books, Mill Valley, CA, 1994; W. Kaim and B. Schwederski, in *Bioinorganic Chemistry*, John Wiley and Sons, Chichester, 1994.

2 A. Volbeda, A. Lahm, F. Sakiyama and D. Suck, *EMBO J.*, 1991, **10**, 1607; E. Hough, L. K. Hansen, B. Birknes, K. Jynge, S. Hansen, A. Hordvik, C. Little, E. Dodson and Z. Derewenda, *Nature* (*London*), 1989, **338**, 357.

3 A. P. Cole, D. E. Root, P. Mukherjee, E. I. Solomon and T. D. P. Stack, *Science*, 1996, **273**, 1848; A. Taylor and W. N. Lipscomb, *J. Mol. Biol.*, 1992, **224**, 141; B. S. Cooperman, A. A. Baykov and R. Lahto, *Trends Biochem. Sci.*, 1992, 262.

4 E. I. Solomon, U. M. Sundaram and T. E. Machonkin, *Chem. Rev.*, 1996, **96**, 2563; A. L. Feig and S. J. Lippard, *Chem. Rev.*, 1994, **94**, 759; A. Messerschmidt, K. Luecke and R. Huber, *J. Mol. Biol.*, 1993, **230**, 997; J. Li, D. R. McMillan and W. E. Antholine, *J. Am. Chem. Soc.*, 1992, **114**, 725; R. Huber, *Angew. Chem.*, *Int. Ed. Engl.*, 1989, **101**, 849.

5 E. Bill, B. Krebs, M. Winter, M. Gerdan, A. X. Trautwein, U. Florke, H.-J. Haupt and P. Chaudhuri, *Chem. Eur. J.*, 1997, **3**, 193; D. M. Kurtz, *Chem. Rev.*, 1990, **90**, 585; J. B. Vincent, G. L. Oliver-Lilley and B. A. Averill, *Chem. Rev.*, 1990, **90**, 1447.

6 F. Birkelbach, U. Florke, H.-J. Haupt, C. Butzlaff, A. X. Trautwein, K. Wieghardt and P. Chaudhuri, *Inorg. Chem.*, 1998, **37**, 2000; R.-D. Schnebeck, L. Randacio, E. Zangrando and B. Lippert, *Angew. Chem.*, *Int. Ed.*, 1998, **37**, 119; J. Barbera, A. Elduque, R. Gimenez, F. J. Lahoz, J. A. Lopez, L. A. Oro and J. L. Serrano, *Inorg. Chem.*, 1998, **37**, 2960; C. J. Jones, *Chem. Soc. Rev.*, 1998, **27**, 289; H. Zhu, Q. Liu, X. Huang, T. Wen, C. Chen and D. Wu, *Inorg. Chem.*, 1998, **37**, 2678; T. Nakamoto, M. Hanaya, M. Katada, K. Endo, S. Kitagawa and H. Sano, *Inorg. Chem.*, 1997, **36**, 4347; F. C. J. M. van Veggel, W. Verboom and D. N. Reinhoudt, *Chem. Rev.*, 1994, **94**, 279; D. Luneau, H. Oshio, H. Okawa and S. Kida, *J. Chem. Soc.*, *Dalton Trans*, 1990, 2283; R. D. Cannon and R. P. White, *Prog. Inorg. Chem.*, 1988, **36**, 195; G. Renger, *Angew. Chem.*, *Int. Ed. Engl.*, 1987, **26**, 643; M. E. Lines, A. P. Ginsberg, R. L. Martin and R. C. Sherwood, *J. Chem. Phys.*, 1972, **57**, 1; K. Sauer, *Acc. Chem. Res.*, 1980, **13**, 249.

7 W. C. Still, *Acc. Chem. Rev.*, 1996, **29**, 155; F. C. J. M. van Veggel, W. Verboom and D. N. Reinhoudt, *Chem. Rev.*, 1994, **94**, 279; H. An, J. S. Bradshaw, R. M. Izatt and Z. Yan, *Chem. Rev.*, 1994, **94**, 939; R. M. Izatt, J. S. Bradshaw, K. Pawlak, R. L. Bruening and B. J. Tarbet, *Chem. Rev.*, 1992, **92**, 1261; K. E. Krakowiak, J. S. Bradshaw and D. J. Zamecka-Krakowiak, *Chem. Rev.*, 1989, **89**, 929.

8 N. H. Pilkington and R. Robson, *Aust. J. Chem.*, 1970, **23**, 2225; R. R. Gagne, C. L. Spiro, T. J. Smith, C. A. Hamann, W. R. Thies and A. K. Shiemke, *J. Am. Chem. Soc.*, 1981, **103**, 4073; P. Guerriero, S. Tamburini and P. A. Vigato, *Coord. Chem. Rev.*, 1995, **139**, 17; H. Aneetha, C. R. K. Rao, K. M. Rao, P. S. Zacharias, X. Feng, T. C. W. Mak, B. Srinivas and M. Y. Chiang, *J. Chem. Soc.*, *Dalton Trans.*, 1997, 1697; J. Reim and B. Krebs, *J. Chem. Soc.*, *Dalton Trans.*, 1997, 3793; G. Alzuet, L. Casella, M. L. Villa, O. Carugo and M. Gullotti, *J. Chem. Soc.*, *Dalton Trans.*, 1997, 4789; M. Ghiladi, C. J. McKenzie, A. Meier, A. K. Powell, J. Ulstrup and S. Wocadlo, *J. Chem. Soc.*, *Dalton Trans.*, 1997, 4011; E. V. Kybak-Akimova, N. W. Alcock and D. H. Busch, *Inorg. Chem.*, 1998, **37**, 1563; S. Mohanta, K. K. Nanda, L. K. Thompson, U. Florke and K. Nag, *Inorg. Chem.*, 1998, **37**, 1465; K. K. Nanda, A. W. Addison, N. Paterson, E. Sinn, L. K. Thompson and U. Sakaguchi, *Inorg. Chem.*, 1998, **37**, 1028; T. Koga, H. Furutachi, T. Nakamura, N. Fukita, M. Ohba, K. Takahashi and H. Okawa, *Inorg. Chem.*, 1998, **37**, 989; A. Asokan, B. Varghese, A. Caneschi and P. T. Manoharan, *Inorg. Chem.*, 1998, **37**, 228; A. Asokan, B. Varghese and P. T. Manoharan, *Inorg. Chem.*, 1999, **38**, 4393; P. E. Kruger, F. Launay and V. McKee, *Chem. Commun.*, 1999, 639; P. Starynowicz and J. Lisowski, *Chem. Commun.*, 1999, 769.

9 P. Zanello, S. Tamburini, P. A. Vigato and G. A. Mazzocchin, *Coord. Chem. Rev.*, 1987, **77**, 165; P. A. Vigato, S. Tamburini and D. E. Fenton, *Coord. Chem. Rev.*, 1990, **106**, 25; P. Guerriero, S. Tamburini and P. A. Vigato, *Coord. Chem. Rev.*, 1995, **139**, 17; S. Uhlenbrock and B. Krebs, *Angew. Chem.*, *Int. Ed. Engl.*, 1992, **31**, 1647; E. Kimura and T. Koike, *Chem. Commun.*, 1998, 1495; S. E. Denmark, S. P. D. Connor and S. R. Wilson, *Angew. Chem.*, *Int. Ed. Engl.*, 1998, **37**, 1149.

10 A. Christensen, H. S. Jensen, V. McKee, C. J. McKenzie and M. Munch, *Inorg. Chem.*, 1997, **36**, 6080; S. S. Tandon, L. K. Thompson, J. N. Bridson and C. Benelli, *Inorg. Chem.*, 1995, **34**, 5507; K. K. Nanda, S. Mohanta, U. Florke, S. K. Dutta and K. Nag, *J. Chem. Soc.*, *Dalton Trans.*, 1995, 3831; B. F. Hoskins, R. Robson and P. Smith, *J. Chem. Soc.*, *Chem. Commun.*, 1990, 488.

11 Y. Tian, J. Tong, G. Frenzen and J.-Y. Sun, *J. Org. Chem.*, 1999, **64**, 1442; A. J. Atkins, D. Black, A. J. Blake, A. Marin-Becerra, S. Parsons, I. Ramirez and M. Schroder, *Chem. Commun.*, 1996, 457.

12 F. Avecilla, R. Bastida, A. de Blas, D. E. Fenton, A. Macias, A. Rodriguez, T. Rodriguez-Blas, S. Garcia-Granda and R. Corzo-suarez, *J. Chem. Soc.*, *Dalton Trans.*, 1997, 409; E. Asato, H. Furutachi, T. Kawahashi and M. Mikuriya, *J. Chem. Soc.*, *Dalton Trans.*, 1995, 3897.

13 S. R. Korupoju and P. S. Zacharias, *Chem. Commun.*, 1998, 1267.

14 Y. L. Bennani and S. Hanessian, *Chem. Rev.*, 1997, **97**, 3161.

15 S. R. Korupoju, N. Mangayarkarasi, P. S. Zacharias, Kumar Biradha and M. Zavorotko, to be communicated.

16 C. K. Johnson, ORTEP II, Report ORNL-5138, Oak Ridge National Laboratory, Oak Ridge, TN, 1976.

17 H. Adams, N. A. Bailey, P. Bertrand, C. O. Rodriguez de Barbarin, D. E. Fenton and S. Gou, *J. Chem. Soc.*, *Dalton Trans.*, 1995, 295.

18 D. Carlisle, D. E. Fenton, P. B. Roberts, U. Casellato, P. A. Vigato and R. Graziani, *Transition Met. Chem.*, 1986, **11**, 292; K. Brychcy, K. Drager, K.-J. Jens, M. Tilset and U. Behrens, *Chem. Ber.*, 1994, **127**, 465; K. Brychcy, K.-J. Jens, M. Tilset and U. Behrens, *Chem. Ber.*, 1994, **127**, 991; C. R. K. Rao and P. S. Zacharias, *Polyhedron*, 1997, **16**, 1201.

19 R. H. Holm, *J. Am. Chem. Soc.*, 1960, **82**, 5632.

20 K. K. Nanda, R. Das, K. Venkatasubramanian, P. Paul and K. Nag, *J. Chem. Soc.*, *Dalton Trans.*, 1993, 2515.

21 C. Fraser, L. Johnston, A. L. Rheingold, B. S. Haggerty, G. K. Williams, J. Whelan and B. Bosnich, *Inorg. Chem.*, 1992, **31**, 1835; M. Mahapatra, V. Chakravorthy and K. C. Dash, *Polyhedron*, 1989, **8**, 1509 and references therein.

22 S. K. Dutta, J. Ensling, R. Werner, U. Florke, W. Haase, P. Gutlich and K. Nag, *Angew. Chem.*, *Int. Ed. Engl.*, 1997, **36**, 152 and references therein.

23 D. Luneau, J.-M. Savariault, P. Cassoux and J.-P. Tuchagues, *J. Chem. Soc.*, *Dalton Trans.*, 1988, 1225; Y. Ikawa, T. Nagata and K. Maruyama, *J. Chem. Soc.*, *Chem. Commun.*, 1994, 471.

24 H. Okawa and S. Kida, *Bull. Chem. Soc. Jpn.*, 1972, **45**, 1759; R. R. Gagne, C. L. Spiro, T. J. Smith, C. A. Hamann, W. R. Thies and A. K. Shiemke, *J. Am. Chem. Soc.*, 1981, **103**, 4073; B. Adhikary, S. K. Mandal and K. Nag, *J. Chem. Soc.*, *Dalton Trans.*, 1988, 935; S. Karunakaran and M. Kandaswamy, *J. Chem. Soc.*, *Dalton Trans.*, 1995, 1851; E. V. Rybak-Akimova, D. H. Busch, P. K. Kahol, N. Pinto, N. W. Alcock and H. J. Clase, *Inorg. Chem.*, 1997, **36**, 510.

25 M. Himmelsbach, R. L. Lintvedt, J. K. Zehetmair, M. Nanny and M. J. Heeg, *J. Am. Chem. Soc.*, 1987, **109**, 8003.

26 L. Ledoux and J. Zyss, *Novel Optical Materials and Applications*, eds. I. C. Khoo, F. Simoni and C. Umeton, John Wiley & Sons, New York, 1997.

27 N. J. Long, *Angew. Chem.*, *Int. Ed. Engl.*, 1995, **34**, 21.

28 S. D. Bella, I. Fragala, I. Ledoux, M. A. Diaz-Garcia and T. J. Marks, *J. Am. Chem. Soc.*, 1997, **119**, 9550.

29 G. Lenoble, P. G. Lacroix, J. C. Daran, S. D. Bella and K. Nakatani, *Inorg. Chem.*, 1998, **37**, 2158.

30 S. K. Kurtz and T. T. Perry, *J. Appl. Phys.*, 1968, **39**, 3798; J. P. Dougherty and S. K. Kurtz, *J. Appl. Crystallogr.*, 1976, **9**, 145.

31 J. J. P. Stewart, MOPAC 93, 2nd edn., Fujitsu Inc., 1993.

32 M. J. S. Dewar, E. G. Zoebisch, E. F. Healy and J. J. P. Stewart, *J. Am. Chem. Soc.*, 1985, **107**, 3092.

33 J. F. Larrow, E. N. Jacobson, Y. Gao, Y. Hong, X. Nie and C. M. Zepp, *J. Org. Chem.*, 1994, **59**, 1939.

34 XTAL 3.5, Users Manual, eds S. R. Hall, G. S. D. King and J. M. Stewart, University of Western Australia, Perth, 1995; G. M. Sheldrick, SHELXS 86, SHELXL 93, Program for Crystal Structure Solution and Refinement, University of Göttingen, 1993; SHELX 97, Program for Crystal Structure Solution and Refinement, University of Göttingen, 1997.